

## ON THE GEOMETRY OF RED BLOOD CELL

BORISLAV ANGELOV and IVAÏLO M. MLADENOV

*Institute of Biophysics, Bulgarian Academy of Sciences,  
Acad. G. Bonchev Street, Block 21, 1113 Sofia, Bulgaria*

**Abstract.** The differential geometry of a normal red blood cell is treated using the Cassinian oval for modelling its profile. In this connection an explicit parametrization via Jacobian elliptic functions of the usual polar coordinates is found. The first and the second fundamental forms, and correspondingly, the Gaussian, mean, and principal curvatures, are derived. The integrals determining the volume, area, cross-section area, and circumference of a red blood cell are evaluated analytically and expressed in a form relevant to the sphere geometry via some correction factors. The free elastic energy  $U$ , associated with the outer bilayer membrane of the cell is integrated and its scale dependence is established. A relation between  $U$  and the surface area correction factor is determined. Approximate formulae, using elementary functions, that should be directly applicable to experimental data are developed.

Plots of these dimensionless parts of volume, area, cross-section area, and circumference are obtained. The sphericity index, homogeneity index, and volume/area ratio associated with the red cell geometry are derived in approximate forms as well.

### 1. Introduction

Red blood cells, or erythrocytes, serve to deliver oxygen to cells via the protein hemoglobin. The description of the form of the Red Blood Cell (RBC) is a subject of a research interest for a long time (cf. Funaki [6] for the early history of the subject). The most precise description now available is that given by the equation of the oval of Cassini (see e. g. Funaki [6], Vayo [20], Canham [1], and Figs 1 and 2). The main difficulty that remain unsolved is that related to the complexity of the mathematical expressions describing quantities of geometric interest. Some preliminary results in this field are provided by Funaki [6] and Vayo [20]. For a researcher that is not prepared

and equipped with a specialized software capable to deal with elliptic functions or numerical integration, it is a frustrating task to perform calculations of RBC geometrical parameters. Furthermore, the complex expressions may obscure important qualitative insights on the RBC geometry.

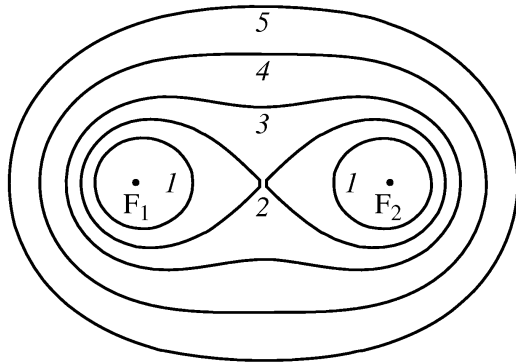


**Figure 1.** RBC shapes at various  $\varepsilon$   
See Sect. 2 for explanation of curves

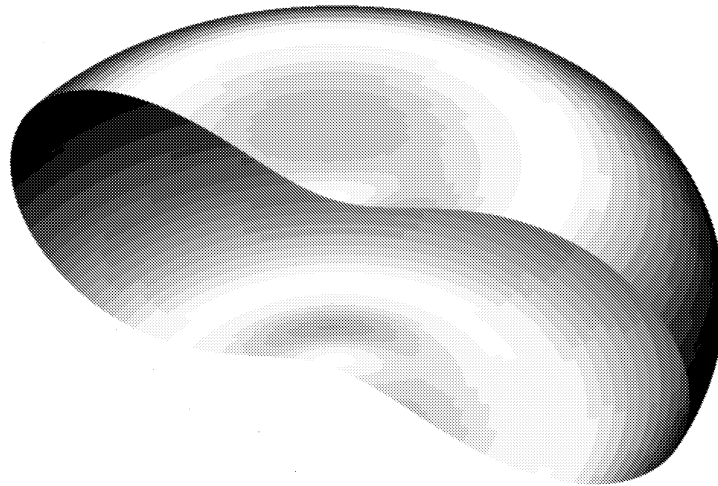


**Figure 2.** A half section of RBC drawn using polar coordinates via elliptic functions

The purpose of this study is to further investigate the expressions of RBC geometry and derive RBC geometrical parameters by applying three new approaches: (1) choosing an appropriate coordinate system, (2) study the relevance of the biconcave shaped RBC form to that of a sphere, and (3) approximating the exact expressions to such that are usable under laboratory conditions. Here, the original formulae are derived for the first and second fundamental forms which specify all kind of curvatures. Having the precise expressions for surface area, volume, cross-section area, and circumference of RBC new expressions are derived which demonstrate their relationship with the corresponding parameters for the ordinary sphere. The exact formulae of the above quantities are approximated to ones suitable for easy practical calculations avoiding the need

of an expensive and sophisticated computer hardware and software.

According to the physical models presented in Canham [1] and Deuling and Helfrich [4] we accept that the geometrical shape of RBC follows the minimization of the elastic energy associated with deformations of the outer membrane of RBC and leads to the geometrical form described by the Cassinian oval. Thus Canham [1] expresses the elastic energy  $U$  as an integral of a special function in the principle curvatures over the membrane surface. Actually its analytical evaluation was considered to be quite difficult and therefore was done numerically.

Our study shows that the geometrical form of RBC based on the Cassinian oval could be determined by experimental measurements of just two parameters, e. g. example its area and volume. At variance, previous publications (cf. Canham [1], Svetina and Zekš [19] and Hwang and Waugh [9]) have considered as insufficient that two such geometrical parameters could determine exactly the RBC form. However, due to practical reasons, the most precise measurements turns out to be that of the diameter  $d$  and the thickness  $\tau$  of RBC. Therefore we consider these experimental parameters as more appropriate input data in the calculations compared to the area, volume and thinness of RBC. We find that knowing  $d$  and  $\tau$  all other geometrical quantities could be easily calculated using the derived approximate expressions in Table 1.

## 2. Explicit Coordinate Presentations of RBC Shape

Following the tradition which can be traced in [1, 4, 6] and [20], we consider the geometrical model of the RBC based on the Cassinian oval (see Fig. 1). This remarkable plane curve is defined as a geometrical locus of the points for which the product of the distances from two fixed points  $\mathbf{F}_1$  and  $\mathbf{F}_2$  is a constant  $c^2$ , when the *distance*  $(\mathbf{F}_1, \mathbf{F}_2)$  between  $\mathbf{F}_1$  and  $\mathbf{F}_2$  is  $2a$ . In the  $XOZ$  plane it is given by the equation

$$(X^2 + Z^2 + a^2)^2 - 4a^2X^2 = c^4. \quad (2.1)$$

It is obvious that the above curve is symmetric with respect to both axes and the origin. Actually its shape depends on the precise relationship of the geometrical parameters  $a$  and  $c$ . Further on we will assume that  $a < c < a\sqrt{2}$  (this case is presented by the curve 3 in Fig. 1). The two cases  $c = a\sqrt{2}$  and  $c > a\sqrt{2}$  produce ellipse like figures illustrated by curves 4 and 5, and the case  $c = a$  gives another well-known curve (2) — the Bernoullian lemniscate

$$(X^2 + Z^2)^2 = 2a^2(X^2 - Z^2), \quad (2.2)$$

while the final case  $a > c$  reduces to two disjoint ovals (curve 1 in Fig. 1).

Cassini has proposed the fourth degree curve (2.1) in an attempt to describe more properly the planetary motion. Both (2.1) and (2.2) are concrete algebraic curves. The general meaning of the last notion is that the rectangular coordinates  $X, Z$  of the points on the curve  $C$  in the plane satisfy an algebraic equation

$$F(X, Z) = 0, \quad (2.3)$$

where  $F(X, Z)$  is a polynomial function in its variables.

As we have already mention all considerations in this work concerns the biconcave disk shape. The later is formed after rotating the contour of the Cassinian oval around the vertical axis. In Cartesian coordinates the RBC surface is described by the equation

$$(a^2 + x^2 + y^2 + z^2)^2 - 4a^2 (x^2 + y^2) = c^4. \quad (2.4)$$

This implicit representation of RBC shape is well-known but from a practical point of view it is nothing more than a definition of a surface in  $\mathbb{R}^3$ . However, in order to describe such object in differential geometry one needs of explicit coordinates, i. e. a triple of smooth functions:

$$x(u, v), \quad y(u, v), \quad z(u, v) \quad (2.5)$$

of two parameters  $(u, v)$  defined in some domain  $D \in \mathbb{R}^2$  and which taken together specify the vector  $\mathbf{x} \in \mathbb{R}^3$

$$\mathbf{x} = \mathbf{x}[u, v] = x(u, v)\mathbf{i} + y(u, v)\mathbf{j} + z(u, v)\mathbf{k}. \quad (2.6)$$

where  $\mathbf{i}, \mathbf{j}, \mathbf{k}$  are the unit vectors along coordinate axes. When  $u$  and  $v$  run in  $D$  the pitch of  $\mathbf{x}$  moves on the surface  $S$ . Below we provide several such parametrizations of RBC surface because each of them is appropriate in a different context.

## 2.1. Polar Coordinates

Let us introduce the standard polar coordinates in the plane

$$x = X \cos \phi, \quad y = X \sin \phi, \quad X \in \mathbb{R}^+, \quad \phi \in [0, 2\pi]. \quad (2.7)$$

Inserting these coordinates into (2.4) and solving it for  $z$  one gets

$$z = \pm \sqrt{\sqrt{c^4 + 4a^2 X^2} - a^2 - X^2}. \quad (2.8)$$

The range interval for  $X$  is  $[0, \sqrt{a^2 + c^2}]$  and the positive(negative) sign corresponds to that part of the surface which is above(below) the polar plane.

## 2.2. Spherical Polar Coordinates

The change of variables in this case is:

$$\begin{aligned}x &= r \sin \theta \cos \phi \\y &= r \sin \theta \sin \phi \\z &= r \cos \theta, \quad r \in \mathbb{R}^+, \quad \theta \in [0, \pi].\end{aligned}$$

and after some work the surface equation (2.4) takes the form

$$r^4 + 2a^2 r^2 \cos 2\theta + a^4 = c^4. \quad (2.9)$$

Again it turns out convenient to solve last equation for  $z = r \cos \theta$  which this time returns

$$z = \pm \frac{\sqrt{c^4 - (a^2 - r^2)^2}}{2a}, \quad r \in [\sqrt{c^2 - a^2}, \sqrt{a^2 + c^2}] \quad (2.10)$$

with the same meaning of signs, and respectively

$$x = \frac{\sqrt{(a^2 + r^2)^2 - c^4}}{2a} \cos \phi, \quad y = \frac{\sqrt{(a^2 + r^2)^2 - c^4}}{2a} \sin \phi. \quad (2.11)$$

## 2.3. Polar Coordinates via Elliptic Functions

Before presenting them we need to introduce some new notation as follows:

$$x^2 + y^2 + z^2 = \rho^2, \quad \lambda^2 = \frac{1}{c^2 + a^2}, \quad \mu^2 = \frac{1}{c^2 - a^2}, \quad (2.12)$$

so that the equation (2.4) becomes

$$4a^2 \lambda^2 \mu^2 z^2 = (1 - \lambda^2 \rho^2)(1 + \mu^2 \rho^2). \quad (2.13)$$

Elsewhere it has been proven (cf. Mladenov [14]) that the uniformization of the algebraic curve

$$w^2 = (1 - \lambda^2 \zeta^2)(1 + \mu^2 \zeta^2) \quad (2.14)$$

is given by the Jacobian elliptic functions as follows

$$\zeta(\tau) = \frac{1}{\sqrt{\lambda^2 + \mu^2}} \frac{sn(\sqrt{\lambda^2 + \mu^2} \tau + F, k)}{dn(\sqrt{\lambda^2 + \mu^2} \tau + F, k)}, \quad (2.15)$$

and

$$w(\tau) = \frac{d}{d\tau} \zeta(\tau) = \frac{cn(\sqrt{\lambda^2 + \mu^2} \tau + F, k)}{dn^2(\sqrt{\lambda^2 + \mu^2} \tau + F, k)}, \quad (2.16)$$

and where the modulus  $k$  of these functions is given by

$$k^2 = \frac{\mu^2}{\lambda^2 + \mu^2} = \frac{c^2 + a^2}{2c^2}, \quad (2.17)$$

while  $F$  is an unspecified for the moment real constant.

Besides, from the very beginning we have assumed as granted  $a < c < a\sqrt{2}$ , and this ensures that the modulus of the elliptic functions  $k$  is less than one (as should be), which means also that we can introduce the complementary modulus  $\tilde{k}$  by the usual formula

$$\tilde{k}^2 = 1 - k^2 = \frac{\lambda^2}{\lambda^2 + \mu^2} = \frac{c^2 - a^2}{2c^2}. \quad (2.18)$$

Now, we can come back to the problem in question, namely that of uniformization of (2.13).

In order to achieve this we assume that the functions  $\rho(u)$  and  $z(u)$  are of the form

$$\rho(u) = \frac{1}{\sqrt{\lambda^2 + \mu^2}} \frac{sn(\sigma u + F, k)}{dn(\sigma u + F, k)}, \quad (2.19)$$

and

$$z(u) = \frac{d}{du} \rho(u) = \frac{\sigma}{\sqrt{\lambda^2 + \mu^2}} \frac{cn(\sigma u + F, k)}{dn^2(\sigma u + F, k)}. \quad (2.20)$$

Entering with (2.19) and (2.20) into (2.13) and taking into account the fundamental functional relationships among Jacobian elliptic functions [11], i. e.,

$$\begin{aligned} sn^2(u, k) + cn^2(u, k) &= 1, \\ dn^2(u, k) &= 1 - k^2 sn^2(u, k) = cn^2(u, k) + \tilde{k}^2 sn^2(u, k), \end{aligned} \quad (2.21)$$

one gets a simple equation about  $\sigma$  that can be easily solved and gives

$$\sigma = \frac{c}{a\sqrt{2}}. \quad (2.22)$$

Up to now the real parameter  $F$  has not been determined. This can be remedied by combining some geometrical and analytical considerations which produce the following transcendental equation

$$dn(F, k) = \frac{1}{\sqrt{2}}. \quad (2.23)$$

Actually, there is not a need to solve it explicitly at this moment as for the relevant computations one can use instead the fundamental identities (2.21) in combination with the existing addition formulae for Jacobian elliptic functions

(cf. [11]). The resulting expressions are enough complicated and will be not reproduced here. Anyway, we will consider further on  $F$  as known quantity.

Taking into account that Cassinian oval is closed, some periodicity condition should be present as well. Due to the mirror symmetry with respect to the horizontal and vertical axes the appropriate choice for the period is  $4T$ , where  $T$  is easily found to be given by the formula

$$T = \frac{K(k) - F}{\sigma}, \quad (2.24)$$

and where

$$K(k) = F\left(\frac{\pi}{2}, k\right) = \int_0^{\pi/2} \frac{d\psi}{\sqrt{1 - k^2 \sin^2 \psi}}, \quad (2.25)$$

is the complete elliptic integral of the first kind.

As a result we have obtained a parametrization of the surface of revolution (2.4)

$$\begin{aligned} x[u, v] &= \sqrt{\rho^2(u) - z^2(u)} \cos v, \\ y[u, v] &= \sqrt{\rho^2(u) - z^2(u)} \sin v, \\ z[u, v] &= z(u), \end{aligned} \quad (2.26)$$

where  $v \in [0, 2\pi]$ ,  $u \in [0, 2T]$  with  $\rho(u)$ ,  $z(u)$  given by (2.19) and (2.20). As a free byproduct we have also the uniformization of the Cassinian oval (2.1) (for more details see Mladenov [15])

$$X = x[u, 0] = x(u), \quad Z = z(u). \quad (2.27)$$

### 3. Fundamental Forms of RBC Surface

Let  $S$  be a smooth surface and  $\mathbf{x} = \mathbf{x}[u, v]$  is its vector equation such that  $\mathbf{x}_u \times \mathbf{x}_v \neq 0$ .

A quadratic differential form

$$I = I[u, v] = ds^2 = d\mathbf{x}^2 = d\mathbf{x} \cdot d\mathbf{x} \quad (3.1)$$

which defines the length element on  $S$  is called the *first fundamental form* of the surface. We have

$$d\mathbf{x} = \mathbf{x}_u du + \mathbf{x}_v dv, \quad d\mathbf{x}^2 = \mathbf{x}_u \cdot \mathbf{x}_u du^2 + 2\mathbf{x}_u \cdot \mathbf{x}_v du dv + \mathbf{x}_v \cdot \mathbf{x}_v dv^2. \quad (3.2)$$

Introducing the standard notation from differential geometry textbooks (see e. g. [16])

$$\begin{aligned} E &= E[u, v] = \mathbf{x}_u \cdot \mathbf{x}_u = \mathbf{x}_u^2, \\ F &= F[u, v] = \mathbf{x}_u \cdot \mathbf{x}_v, \\ G &= G[u, v] = \mathbf{x}_v \cdot \mathbf{x}_v = \mathbf{x}_v^2, \end{aligned} \quad (3.3)$$

the first fundamental form can be rewritten succinctly as follows

$$I = E du^2 + 2F du dv + G dv^2. \quad (3.4)$$

Of no less importance for the theory of the surfaces is the *second fundamental form*

$$II = II[u, v] = d^2\mathbf{x} \cdot \mathbf{n} \quad (3.5)$$

where  $d^2\mathbf{x}$  is the second differential of the radius-vector

$$d^2\mathbf{x} = \mathbf{x}_{uu} du^2 + 2\mathbf{x}_{uv} du dv + \mathbf{x}_{vv} dv^2 + \mathbf{x}_u d^2u + \mathbf{x}_v d^2v, \quad (3.6)$$

and  $\mathbf{n}$  is the normal to  $S$  vector of unit length

$$\mathbf{n} = \mathbf{n}[u, v] = \frac{\mathbf{x}_u \times \mathbf{x}_v}{|\mathbf{x}_u \times \mathbf{x}_v|}. \quad (3.7)$$

The standard notation for the coefficients of the second fundamental form are

$$\begin{aligned} L &= L[u, v] = \mathbf{x}_{uu} \cdot \mathbf{n}, \\ M &= M[u, v] = \mathbf{x}_{uv} \cdot \mathbf{n}, \\ N &= N[u, v] = \mathbf{x}_{vv} \cdot \mathbf{n}, \end{aligned} \quad (3.8)$$

so that

$$II = L du^2 + 2M du dv + N dv^2. \quad (3.9)$$

By definition the *normal curvature*  $\mathbf{k}_n$  in direction  $(du : dv)$  is

$$\mathbf{k}_n = \frac{II}{I} = \frac{L du^2 + 2M du dv + N dv^2}{E du^2 + 2F du dv + G dv^2}, \quad (3.10)$$

and the directions at which it attains extremal values (maximum and minimum) are called *principal*.

**Remark:** If the coordinate curves coincide with the principal directions then

$$F = M \equiv 0, \quad (3.11)$$



and the respective curvatures of these directions can be found by the formulae (cf. [7])

$$\mathbf{k}_1 = \frac{L}{E}, \quad \mathbf{k}_2 = \frac{N}{G}. \quad (3.12)$$

We have found that the spherical polar coordinates and the polar coordinates expressed via Jacobian elliptic functions are more appropriate for the purposes of differential geometric considerations as they lead to the most simple formulae in this context. Let us remark also that actually  $r \equiv \rho$ , a fact which was implicit in our considerations up to now. Applying the recipes given above one can arrive at the following results:

$$\begin{aligned} E &= \frac{2c^2\rho^4}{(\rho^2 + a^2)^2 - c^4}, \quad F = 0, \quad G = \frac{(\rho^2 + a^2)^2 - c^4}{4a^2}, \\ L &= \frac{\rho(3\rho^4 + a^4 - c^4)}{(\rho^2 + a^2)^2 - c^4}, \quad M = 0, \quad N = \frac{(\rho^2 - a^2)((\rho^2 + a^2)^2 - c^4)}{4a^2c^2\rho}, \end{aligned} \quad (3.13)$$

and respectively

$$\mathbf{k}_1 = \frac{3\rho^4 + a^4 - c^4}{2c^2\rho^3}, \quad \mathbf{k}_2 = \frac{\rho^2 - a^2}{c^2\rho}. \quad (3.14)$$

Classical differential geometry operates also with other important notions which are of immediate interest for us. These are the Gaussian curvature

$$K = \mathbf{k}_1 \cdot \mathbf{k}_2 = \frac{(\rho^2 - a^2)(3\rho^4 + a^4 - c^4)}{2c^4\rho^4}, \quad (3.15)$$

the mean curvature

$$H = \frac{\mathbf{k}_1 + \mathbf{k}_2}{2} = \frac{(\rho^2 - a^2)^2 + 4\rho^4 - c^4}{4c^2\rho^3}, \quad (3.16)$$

and the surface area element

$$dA = \sqrt{EG - F^2} du dv = \sqrt{EG} du dv = \frac{c}{a\sqrt{2}} \rho^2 du dv. \quad (3.17)$$

**Remark:** The principal curvatures can be expressed in terms of  $K$  and  $H$  as well, and the precise relationships are

$$\mathbf{k}_1 = \mathbf{k}_+ = H + \sqrt{H^2 - K}, \quad \mathbf{k}_2 = \mathbf{k}_- = H - \sqrt{H^2 - K}, \quad (3.18)$$

with selfexplanatory meaning of the subscript indices. Besides, it should be noted also that  $\mathbf{k}_1$  and  $\mathbf{k}_2$  are the principal curvatures along the meridians and parallels of latitude respectively.

## 4. Geometric Quantities of RBC

By both analytical and numerical reasons it turns out more convenient to work instead of original variables  $a$  and  $c$ , with the dimensionless ratio  $\varepsilon = a/c$  and  $c$ . All formulae are expressed in the form relevant to the sphere of radius  $c$ , i. e. the respective result for this sphere multiplied by a *correction factor* that is dependent on  $a/c$  ratio. The range of  $\varepsilon$  is  $\left[\frac{1}{\sqrt{2}}, 1\right]$ . The importance of these geometric quantities is discussed elsewhere (see e. g. Funaki [6] or Vayo [20]).

### 4.1. Diameter and Thickness

The diameter  $d$  of RBC expressed via  $(a, c)$  or  $(c, \varepsilon)$  is

$$d = 2\sqrt{a^2 + c^2} = 2c\sqrt{1 + \varepsilon^2}. \quad (4.1)$$

The thickness denoted by  $\tau = 2z_{\max}$  is attained at  $x(z_{\max})$ , where

$$z_{\max} = \frac{c^2}{2a} = \frac{c}{2\varepsilon}, \quad x(z_{\max}) = \sqrt{a^2 - z_{\max}^2} = \frac{\sqrt{4a^4 - c^4}}{2a}, \quad (4.2)$$

and in order that this is a real coordinate one should have the preassumed inequality  $a\sqrt{2} > c$ . The last obvious geometric characteristic of the Cassinian oval is its thinness given by  $t = 2z_{\min}$  at  $x(z_{\min}) = 0$ ,

$$z_{\min} = \sqrt{c^2 - a^2} = c\sqrt{1 - \varepsilon^2}. \quad (4.3)$$

The diameter and thickness can be measured experimentally using photographed red cell profiles or electron micrographs [5]. The useful links between them and the mathematical constants  $a, c$  are given by the formulae

$$a = \frac{\sqrt{d^2 + \tau^2} - \tau}{2}, \quad c = \frac{\sqrt{\tau\sqrt{d^2 + \tau^2} - \tau^2}}{\sqrt{2}}, \quad (4.4)$$

$$\varepsilon = \frac{\sqrt{\tau\sqrt{d^2 + \tau^2} - \tau^2}}{\tau\sqrt{2}}, \quad c = \varepsilon\tau.$$

The choice of  $d$  and  $\tau$  as a set of sufficient experimentally measurable quantities was made on the basis of the smallest errors in comparison with other potential choices. Actually, the experimental errors when measuring  $d$  and  $\tau$  are less than 5% as reported in [2]. Relying on (4.4) and (4.1) one easily find the relation between  $d$  and  $\tau$  to be

$$d = 2\tau\varepsilon\sqrt{1 + \varepsilon^2}. \quad (4.5)$$

Since  $\varepsilon$  varies between  $\frac{1}{\sqrt{2}}$  and 1, the range of  $d$  is in the interval  $[\sqrt{3}\tau, 2\sqrt{2}\tau]$ .

### 4.2. Volume

The volume of RBC is obtained by combining the shell method and the polar coordinates (2.7) which produce the integral

$$\text{Volume} = V = 4\pi \int_0^{\sqrt{a^2+c^2}} Xz(X) dX, \tag{4.6}$$

The result is

$$V = \frac{4}{3}\pi c^3 V(\varepsilon), \tag{4.7}$$

where the dimensionless correction factor  $V(\varepsilon)$  is

$$V(\varepsilon) = \frac{\sqrt{1-\varepsilon^2}(1+2\varepsilon^2)}{4} + \frac{3\arccos(1-2\varepsilon^2)}{8\varepsilon}. \tag{4.8}$$

Figure 3 shows the plot of  $V(\varepsilon)$  vs.  $\varepsilon$ . In contrast to other quantities considered below, the volume has inflection. The difference between minimal and maximal values is smaller than the other geometric quantities have.

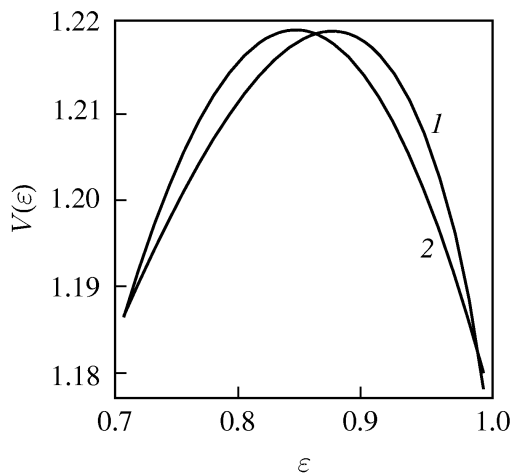


**Figure 3.** Volume correction vs.  $\varepsilon$  (curve 1) and its approximation (curve 2)

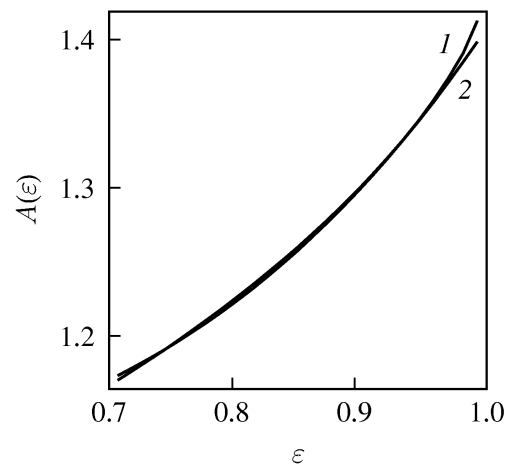


**Figure 4.** Area correction vs.  $\varepsilon$  (curve 1) and its approximation (curve 2)

### 4.3. Surface Area

Many important physiological processes performed by RBC, and especially the gas exchange, depend on the magnitude of its surface area. Relying this time on the spherical polar coordinates (2.9) it can be written as the integral

$$\text{Area} = A = 4\pi \int_0^{\sqrt{a^2+c^2}} X \, ds(X) = 4\pi \int_{\sqrt{c^2-a^2}}^{\sqrt{a^2+c^2}} \rho \sin(\tilde{\theta}) \, ds(\rho), \quad \tilde{\theta} \in [0, \pi/2], \quad (4.9)$$

where the infinitesimal arclength  $ds(\rho)$  along the Cassinian oval (2.1) is found by Matz [13] to be

$$ds(\rho) = \frac{2c^2 \rho^2 \, d\rho}{\sqrt{[(\rho^2 + a^2)^2 - c^4][c^4 - (\rho^2 - a^2)^2]}}. \quad (4.10)$$

Actually this result can be derived much more easily if one makes use of the parametrization given by (2.10) and (2.11). Performing the integration we have

$$A = 4\pi c^2 A(\varepsilon). \quad (4.11)$$

with a correction factor

$$A(\varepsilon) = \frac{\sqrt{2}}{\varepsilon} \left[ E \left( \arccos \sqrt{\frac{1-\varepsilon^2}{1+\varepsilon^2}}, \sqrt{\frac{1+\varepsilon^2}{2}} \right) - \frac{1-\varepsilon^2}{2} F \left( \arccos \sqrt{\frac{1-\varepsilon^2}{1+\varepsilon^2}}, \sqrt{\frac{1+\varepsilon^2}{2}} \right) \right]. \quad (4.12)$$

Here  $F(\psi, k)$  and  $E(\psi, k)$  denote the first, and respectively the second kind of incomplete elliptic integrals. Their definition and properties can be found e. g. in Jahnke *et al.* [11]. Figure 4 shows the plot of  $A(\varepsilon)$  vs.  $\varepsilon$ , which is obviously a monotonically increasing function of  $\varepsilon$ .

### 4.4. Cross Section Area

Due to the rotational symmetry of the RBC we were able to reduce the evaluation of its volume and area to single integration. In the case of the cross-section area it is a matter of definition to write

$$\text{Cross Section Area} = A_C = 4 \int_0^{\sqrt{a^2+c^2}} z(X) \, dX, \quad (4.13)$$

and to obtain

$$A_C = \pi c^2 A_C(\varepsilon) \quad (4.14)$$

with a correction factor

$$A_C(\varepsilon) = \frac{2E(\varepsilon^2)}{\pi}, \quad (4.15)$$

where  $E(k) = E(\pi/2, k)$  is the complete elliptic integral of the second kind. Figure 5 shows the plot of  $A_C(\varepsilon)$  vs.  $\varepsilon$ . In contrast to the surface area, the cross-section area correction decreases when  $\varepsilon$  approaches the right end of its interval of definition.

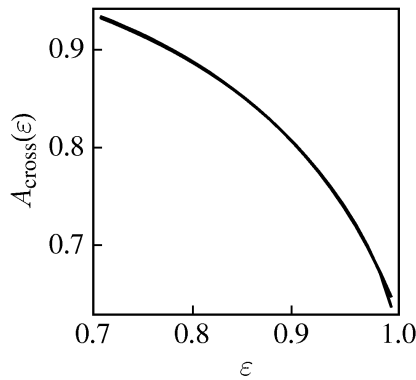


**Figure 5.** Correction of cross section area

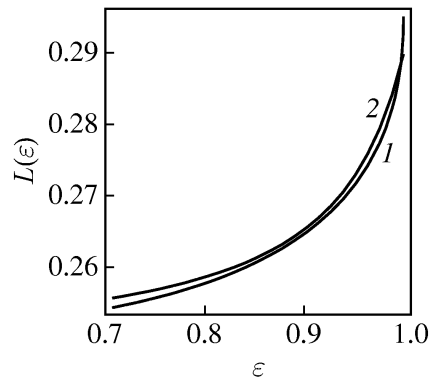


**Figure 6.** Correction of cross section length

#### 4.5. Length of Cross Section

The circumference of the Cassinian oval can be obtained by performing the integration

$$\text{Circumference} = L = \int ds = 2\pi cL(\varepsilon) \quad (4.16)$$

where the infinitesimal arclength  $ds$  along the red cell contour (2.1) is specified in (4.10) and the correction factor is

$$L(\varepsilon) = \frac{{}_2F_1\left(\frac{1}{4}, \frac{1}{2}, 1, m\right)}{4\sqrt{1+\varepsilon^2}}. \quad (4.17)$$

Here  ${}_2F_1(\alpha, \beta, \gamma, m)$  is the non-degenerated Gauss hypergeometric function with parameters  $\alpha = 1/4$ ,  $\beta = 1/2$ ,  $\gamma = 1$  and  $m(\varepsilon) = m = \frac{2\varepsilon}{1+\varepsilon^2}$  is its argument. Figure 6 shows the plot of  $L(\varepsilon)$  vs.  $\varepsilon$ . When  $\varepsilon$  approaches 1, the circumference factor increases rapidly.

## 5. Elastic Free Energy of RBC Outer Membrane

According to Canham [1] the elastic energy of bending is

$$U = \frac{D}{2} \int (k^2_+ + k^2_-) dA \quad (5.1)$$

where  $D$  is the bending rigidity constant. Integration (up to the scaling factor  $\frac{D}{2}$ ) results in:

$$U(\varepsilon) = \frac{28}{3} \pi - \frac{2}{3} \pi \left( 8 + \frac{1}{\varepsilon^2} - 12\varepsilon^2 \right) T + \frac{32\sqrt{2}}{3} \pi \varepsilon |E(k) - E(\varphi, k)| \quad (5.2)$$

where  $\varphi$  called *amplitude*, is defined by

$$\varphi = am(F, k), \quad F = F(\varphi, k) = \int_0^\varphi \frac{d\psi}{\sqrt{1 - k^2 \sin^2 \psi}}, \quad (5.3)$$

and

$$k^2 = \frac{1 + \varepsilon^2}{2}.$$

**Remark:** The last equation does not mean that  $F$  from (2.23) and the incomplete elliptic integral  $F(\varphi, k)$  are identical, but just provides a definition of the amplitude  $\varphi$ .

Graphically  $U(\varepsilon)$  is plotted in Fig. 10. Toward  $\varepsilon = 1$  its value is almost duplicated.

The surface area  $A$  can be obtained also by integration of  $\sqrt{EG}$  and this gives

$$A = 4\pi c^2 A(\varepsilon) = \int dA = \int_0^{2\pi} dv \int_0^{2T} \sqrt{EG} du, \quad (5.4)$$

with

$$A(\varepsilon) = 1 + \frac{(\varepsilon^2 - 1)}{2\varepsilon^2} T + \frac{\sqrt{2}}{\varepsilon} |E(k) - E(\varphi, k)|, \quad (5.5)$$

and where use has been made of (3.17), (2.19) and (2.24). The relation between  $U(\varepsilon)$  and  $A(\varepsilon)$  was found to be:

$$U(\varepsilon) = \frac{4}{3} \pi [7 + 8(A(\varepsilon) - 1)\varepsilon^2] + \frac{2\pi(4\varepsilon^4 - 1)}{3\varepsilon^2} T \quad (5.6)$$

This demonstrates the  $\varepsilon$  dependence of the free elastic energy and emphasize the importance of the form in comparison with the size of RBC.

**Remark:** Recently Liu *et al.* [12] have shown, that using elastic energy function which depends on the so called Helfrich spontaneous curvature  $c_0$ , the biconcave shape of RBC turns out to be with a minimal elastic energy attained at  $c_0 = 1.2$ . This shape corresponds to the one described by a Cassinian oval with  $\varepsilon = 0.843$ . Further investigation on correspondence between Cassinian oval and shapes resulting from Helfrich energy minimization procedure is quite tempting.

## 6. Approximate Formulae

The next step towards simplification of the geometric expressions is to approximate the  $\varepsilon$  dependent parts. The main idea is to eliminate the elliptic functions that appear in the exact formulae. Procedures used for numerical approximation are presented elsewhere in the standard texts on numerical methods like [17].

**Table 1.**

Quantity	Expression	Approximation
Volume	$\frac{4}{3} \pi c^3 V(\varepsilon)$	$V(\varepsilon) = (2.88 - 1.7\varepsilon)\varepsilon$
Surface Area	$4\pi c^2 A(\varepsilon)$	$A(\varepsilon) = \frac{2.88 - 1.7\varepsilon}{2.82 - 1.98\varepsilon}$
Area of Cross Section	$\pi c^2 A_C(\varepsilon)$	$A_C(\varepsilon) = \frac{1.05 - 0.94\varepsilon}{1 - 0.83\varepsilon}$
Circumference	$2\pi c L(\varepsilon)$	$L(\varepsilon) = \frac{2.5 - 2.3\varepsilon}{10 - 9.31\varepsilon}$
Elastic Free Energy	$\frac{D}{2} U(\varepsilon)$	$U(\varepsilon) = \frac{151.3 - 148.23\varepsilon}{10 - 17.21\varepsilon + 7.25\varepsilon^2}$
Sphericity	$\sqrt[3]{36\pi} \frac{V^{\frac{2}{3}}}{A} = \frac{[V(\varepsilon)]^{\frac{2}{3}}}{A(\varepsilon)}$	$\frac{[V(\varepsilon)]^{\frac{2}{3}}}{A(\varepsilon)} = \frac{10.38 - 8.8\varepsilon}{10 - 8\varepsilon}$
Homogeneity	$\frac{1}{6\sqrt{\pi}} \frac{A^{\frac{3}{2}}}{V} = \frac{[A(\varepsilon)]^{\frac{3}{2}}}{V(\varepsilon)}$	$\frac{[A(\varepsilon)]^{\frac{3}{2}}}{V(\varepsilon)} = \frac{0.95 - 0.75\varepsilon}{1 - 0.86\varepsilon}$
Volume/Area	$\frac{V}{A} = \frac{c}{3} \frac{V(\varepsilon)}{A(\varepsilon)}$	$\frac{V(\varepsilon)}{A(\varepsilon)} = (2.82 - 1.98\varepsilon)\varepsilon$
Circumference/Area	$\frac{L}{A} = \frac{1}{2c} \frac{L(\varepsilon)}{A(\varepsilon)}$	$\frac{L(\varepsilon)}{A(\varepsilon)} = \frac{29 - 28.38\varepsilon}{100 - 50\varepsilon - 47\varepsilon^2}$
$\frac{\text{Volume}}{\text{Area}} \frac{\text{Circumference}}{\text{Area}}$	$\frac{VL}{A^2} = \frac{1}{6} \frac{V(\varepsilon)L(\varepsilon)}{[A(\varepsilon)]^2}$	$\frac{V(\varepsilon)L(\varepsilon)}{[A(\varepsilon)]^2} = 0.341 - 0.168\varepsilon$

The above Table 1 presents the approximated formulae within the valid range of  $\varepsilon \in \left[ \frac{1}{\sqrt{2}}, 0.998 \right]$  where the error of approximation is near 1%. The  $\varepsilon$  dependent factor in the volume expression contribute nearly 20%. Within 2% accuracy  $V(\varepsilon) = 1.2$ . It is interesting to note that the volume has maximum at  $\varepsilon \approx 7/8$ . On the basis of these approximations one can easily derive relations between any two listed items. This is almost obvious because if any two of them are known, i. e. their values were measured with enough precision, the rest can be obtained also using these approximations.

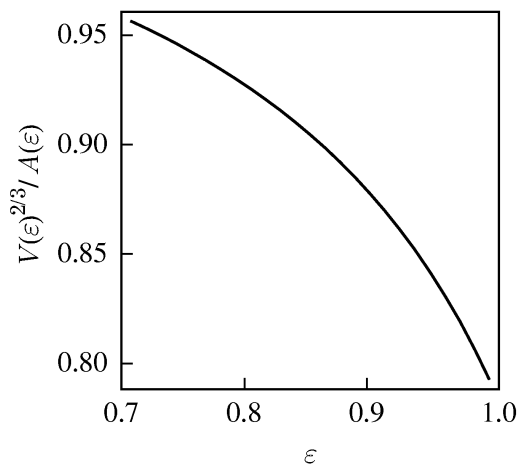


**Figure 7.** Sphericity index vs.  $\varepsilon$  (cf. [1])

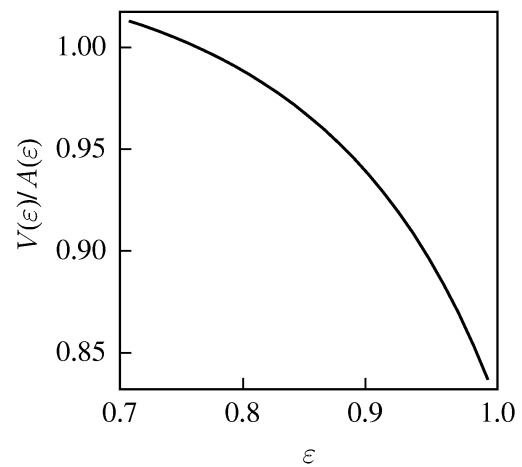


**Figure 8.** Volume/area vs.  $\varepsilon$

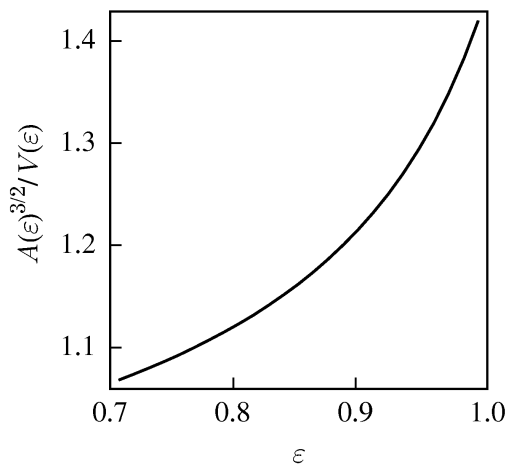


**Figure 9.** Homogeneity index vs.  $\varepsilon$  (cf. [10])

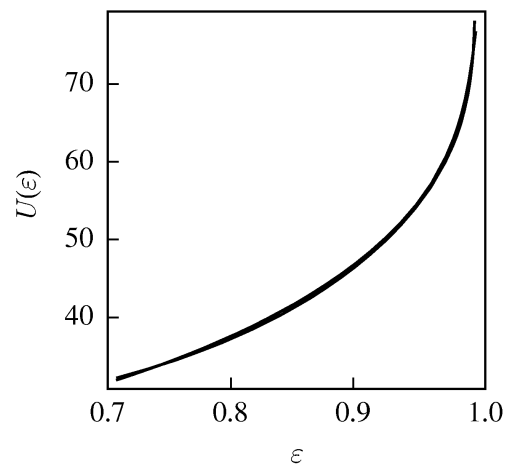


**Figure 10.** Free energy vs.  $\varepsilon$

Figures 8 and 12 represent  $\varepsilon$  dependence of  $V(\varepsilon)/A(\varepsilon)$ , and  $L(\varepsilon)/A(\varepsilon)$  respectively.



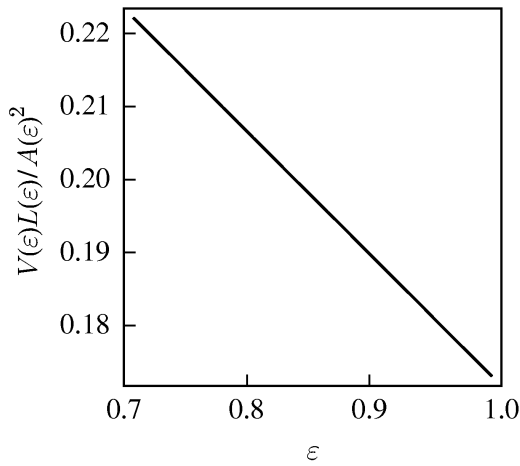


**Figure 11.**  $VL/A^2$  vs.  $\varepsilon$

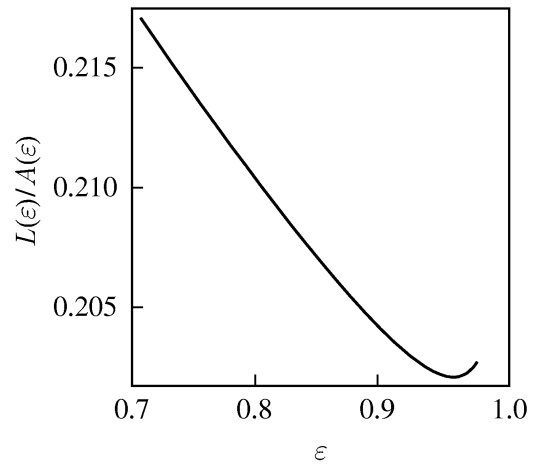


**Figure 12.** Circumference/area vs.  $\varepsilon$

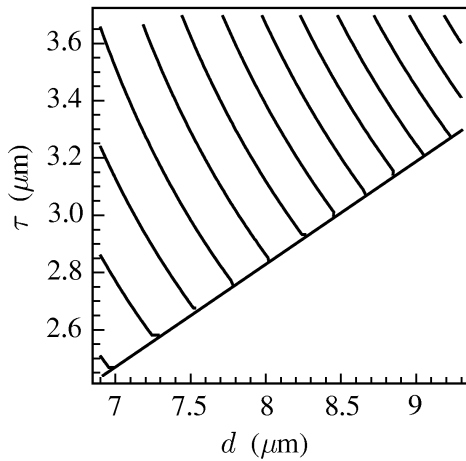


**Figure 13.** Constant volume curves  $V(d,\tau)$

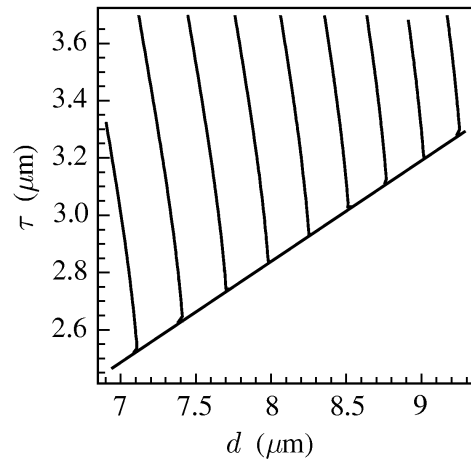


**Figure 14.** Constant area curves  $A(d,\tau)$

## 7. Concluding Remarks

Experimental measurements of the diameter and the thickness of RBC reveal ranges from 6.9 to 9.3  $\mu\text{m}$ , and from 2.4 to 3.7  $\mu\text{m}$  respectively [2]. In Figs 13 and 14 (left-up corners) are represented the possible volumes and surface areas as functions of  $c$ , and  $\varepsilon$ , or what is the same, as functions of  $d$  and  $\tau$ . The minimal volume and surface area are observed when  $d = 6.9 \mu\text{m}$  and  $\tau = 2.44 \mu\text{m}$ . The maximal values are achieved when  $d = 9.3 \mu\text{m}$  and  $\tau = 3.7 \mu\text{m}$ . The parallel curves there represent equal volumes or surface areas. They vary from 73 to 200  $\mu\text{m}^3$  for the volume and from 104.7 to 193.3  $\mu\text{m}^2$  for the surface area. Lower right parts of these graphics are empty since such combination of  $d$ 's and  $\tau$ 's could not exist due to the requirement  $\varepsilon < 1$ . Calculations of the

ranges of  $c$  and  $\varepsilon$  result in the interval from 2.44 to 3.41  $\mu\text{m}$  for  $c$ , and from 0.747 to 1 for  $\varepsilon$ .

In Figures 7, 9 and 11 are shown various indices which are dimensionless and indicate the relevance of the RBC form to the sphere.

## Appendix

Majority of research in the field of Biophysics is devoted to the investigation of molecules of biological interest. Fortunately all of the biological molecules are *polymers* and can be divided in four major groups. Namely, these groups are nuclear acids, proteins, lipids, and sugars [8]. Our contribution here considers lipids. Their unique property is that they form periodic phases when mixed with water. The lipid molecules do not really mix with water molecules, but arrange to built well defined separation walls, the so called *interfaces*.

Development of power X-ray diffraction techniques, especially X-ray synchrotron radiation, drive the development of the subject of lipid/water polymorphism [18]. Another physical experimental method giving structural information is the magnetic resonance. By these experimental techniques it was found that lipid/water phases can be of one-, two-, or three-dimensional periodicity, and that they are kind of *liquid crystals*.

Also unique property is that by simple variation of the temperature or composition of the system, the number of phases which lipid/water system pass exceeds the number of possible phases of any other kind of molecules known. This makes lipid/water phases an attractive object of research in the field of structural *phase transitions*. From theoretical physics point of view the theory that describes lipid/water phase is the statistical mechanics complemented by the mechanics of elastic continuous media. According to the Landau theory of phase transitions, it is possible to describe a given transition by introducing the so called order parameter(s), and on this base to find the minimum of the free energy of the thermodynamic system, where the system is supposed to have an equilibrium. Because of the presence of the interfaces between lipid and water molecules the *principal curvatures* of these interfaces are found to be the most appropriate order parameters. Again there was a good surprise that lipid/water interfaces prefer to have constant mean curvature for all the single equilibrium phases. A particular case is when the mean curvature is zero, i. e., lipid/water interface is described by a minimal surface [3].

At the next level of specialization, we fix our attention to the outer membrane of RBC. This membrane originates from the family of one-dimensional periodic phases, called lamellar. The membrane is constituted of two lipid layers surrounded by water. The involved lipid molecules have electrostatic polar

and non polar parts. They orient themselves with the polar part toward water, just like dipole in an external  $EM$  field. The diameter of RBC is nearly  $8 \mu\text{m}$ , which compared to 15–20 nm thickness of the bilayer membrane, make it almost locally flat surface.

The form of the RBC is given by the contour of the outer membrane. As investigated thoroughly, curvatures play a vital role in describing the behavior of cell membranes, model lipid bilayers, lipid/water phases, etc., and the results presented here give just another example.

### Acknowledgement

This work was partially supported by the National Science Fund of the Bulgarian Ministry of Education and Science, Grant No F-644/1996.

### References

- [1] Canham P., *The Minimum Energy of Bending as a Possible Explanation of the Biconcave Shape of the Human Red Blood Cell*, J. Theor. Biol. **26** (1970) 61–81.
- [2] Canham P. and Burton A., *Distribution of Size and Shape in Population of Normal Human Red Cells*, Circulation Res., **22** (1968) 405–416.
- [3] David F., *Geometry and Field Theory of Random Surfaces and Membranes*, In: Statistical Mechanics of Membranes and Surfaces, Nelson D, Piran T. and Weinberg S. (Eds), World Scientific, Singapore 1989.
- [4] Deuling H. and Helfrich W., *Red Blood Cell Shapes as Explained on the Basis of Curvature Elasticity*, Biophys. J. **16** (1976) 861–868.
- [5] Evans E. and Fung Y., *Improved Measurements of the Erythrocyte Geometry*, Microvasc. Res., **4** (1972) 335–347.
- [6] Funaki H., *Contribution on the Shapes of Red Blood Corpuscles*, Japan. J. Physiol., **5** (1955) 81–92.
- [7] Henderson D., *Differential Geometry: A Geometric Introduction*, Prentice Hall, New Jersey, 1998.
- [8] Hoppe W., Lohmann W., Markl H. and Ziegler H. (Eds), *Biophysics*, Springer-Verlag, Berlin 1983.
- [9] Hwang W. and Waugh R., *Energy of Dissociation of Lipid Bilayer From The Membrane Skeleton of Red Blood Cells*, Biophys. J. **72** (1997) 2669–2678.
- [10] Hyde S., Anderson S., Larson K., Blum Z., Landh T., Lidin S. and Ninham B., *The Language of Shape*, Elsevier, Amsterdam 1997.
- [11] Jahnke E, Emde F. and Lösch F., *Tafeln Höherer Funktionen*, Teubner Verlag, Stuttgart 1960.
- [12] Liu Q-H., Haijun Zh., Liu J-X. and Zhong-Can O-Y., *Spheres and Prolate and Oblate Ellipsoids From Analytical Solution of Spontaneous Curvature Fluid Membrane Model*, Preprint, Cond-Mat/9906038, 1999.
- [13] Matz F., *The Rectification of the Cassinian Oval by Means of Elliptic Functions*, Am. Math. Monthly, **2** (1895) 221–222.

- [14] Mladenov I., *An Integrable System on  $\mathbb{S}^2$* , In: Topics in Complex Analysis, Differential Geometry and Mathematical Physics, S. Dimiev and K. Sekigawa (Eds), World Scientific, Singapore 1997, pp. 158–164.
- [15] Mladenov I., *Uniformization of the Cassinian Oval*, C. R. Acad. Sci. Bulg., **53** (2000) 13-16.
- [16] Oprea J., *Differential Geometry and Its Applications*, Prentice Hall, New Jersey, 1997.
- [17] Press W., Flannery B., Teukolsky, and Vetterling W., *Numerical Recipes in Pascal*, Cambridge University Press, Cambridge 1989.
- [18] Seddon J., Templer R., In: *Handbook of Biological Physics Vol. I*, Lipowsky R. and Sackmann E. (Eds), Elsevier, Amsterdam 1995.
- [19] Svetina S. and Zekš B., *Membrane Bending Energy and Shape Determination of Phospholipid Vesicles and Red Blood Cells*, Eur. Biophys. J. **17** (1989) 101–111.
- [20] Vayo H., *Some Red Blood Cell Geometry*, Canadian J. Physiol. Pharmacol., **61** (1983) 646–649.